Thermal Simulation of Hydration Heat in Slab of Taishan Nuclear Power Plant Unit 2

Feng QIN [1*], Feng FAN [1], Zheng LI [2], Hongliang QIAN [1], and Xiaofei JIN [3]

[1] School of Civil Engineering, Harbin Institute of Technology, Haihe Road 202#, Harbin City, Heilongjiang Province, 150090, China
[2] China Construction Second Engineering Bureau Co. Ltd. Nuclear Power Construction Branch, Shenzhen City, Guangdong Province, 518034, China
[3] China State Construction Technical Center, Beijing, 101300, China

ABSTRACT

Taishan nuclear power plant is the third one under construction of European Pressurized Reactor (EPR). To more accurately simulate hydration temperature field in the slab of Taishan nuclear power plant unit 2, the Equivalent Age-Hydration Degree Curve (EAHDC) was developed and was used in combination with the Model Change Interaction Function (MCIF) of ABAQUS to consider effects of age, temperature and construction process on hydration thermal field of concrete. Given the characteristics of construction process and geometry of the slab, half model was adopted to predict hydration temperature field of the whole slab, and MCIF was used to simulate the construction process. With combination of EAHDC and MCIF, the thermal properties of concrete were practically defined as a function of age, temperature, and construction process. Compared with the onsite measured temperature and the simulation temperature without consideration of construction process, the EAHDC-MCIF combination method provides improved accuracy in the simulation of hydration temperature field of concrete.

INTRODUCTION

Taishan Nuclear power plant is the third one under construction of European Pressurized Reactor(EPR) type, which has an enclosed space comprised of slab and double containment as shown in Fig. 1 to prevent radioactive material leakage(Weisshäupl 1999, Dimmelmeier et al. 2012). The slab of Taishan nuclear power plant unit 2 is a reinforced concrete cylinder with depth of 3.8 m and radius of 27.8 m. With a huge concrete volume of 9266 m^3, the slab was divided into 37 oblique construction layers as shown in Fig. 2. Because of the huge volume and consecutive casting, the resulting thermal field and thermal stress field due to cement hydration posed as threat to the quality of concrete.

Base on large set of experimental data, Zhu (2003) proposed computing model for the adiabatic tests with effects of age and temperature. Based on equivalent age and activation energy, Zhang et al. (2003) proposed hyperbolic curve model for adiabatic tests. Based on normalized affinity of hydration reaction, Benboudjema and Torrenti (2008) simulated thermal field and thermal stress of a nuclear containment

using adiabatic test, but some discrepancies exist between the simulated results and the measured data. Concrete composite and construction practice may vary and have considerable impact, which leads to difficulty in determining proper value for parameter of these models.

In order to consider effects of age and temperature on hydration rate and to take full advantage of adiabatic test, equivalent age-hydration degree curve (EAHDC) is used to specify heat generation rate of hydration reaction, which is implemented by using HETVAL, a users' subroutine of ABAQUS written in Fortran to provide internal heat generation in heat transfer analysis (Simulia 2009). The model change interaction function(MCIF) provided by ABAQUS is adopted to simulate construction process.

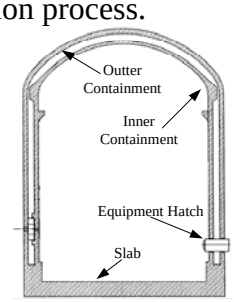

Fig. 1 Double containment and slab of EPR

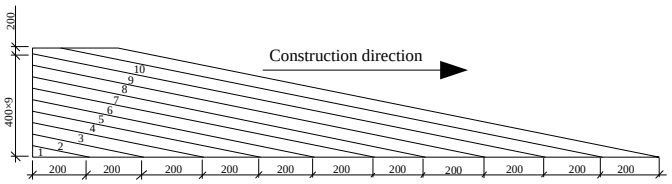

Fig. 2 Oblique construction layers of the slab

EAHDC-MCIF COMBINATION METHOD

Equivalent age-hydration degree curve(EAHDC). Prime cause of temperature increasing of concrete is the hydration heat of cement, adiabatic temperature rise process of concrete is a direct expression of hydration reaction process. If the variation of concrete volume and specific heat is neglected, process of adiabatic temperature rise and process of hydration reaction are synchronous. So hydration status can be predicted according to adiabatic status. Hydration degree at a time point can be defined as the ratio of quantity of cement already has hydrated by this time point and the total quantity of cement can be hydrated at last (WANG et al. 2005). Accordingly, in adiabatic test, hydration degree $\alpha(t)$ can be redefined as the ratio of temperature rise at time t and the maximum adiabatic temperature rise as shown in Eq. (1), where $T_{ad}(t)$ is adiabatic temperature at time t, $T_{ad}(\infty)$ is the maximum adiabatic temperature, and T_0 is initial temperature.

The equal age concept can be used to determine hydration process at different temperature. The basis of equal age concept is the transformation of hydration time in any temperature to hydration time in unified reference temperature T_r. In time peroid Δt, k_c and k_r are hydration rate at temperature $T_c(t)$ and T_r respectively. T_r is constant such as 20 ℃, and $T_c(t)$ vary with time is the actual temperature in concrete during hydration. Hydration reaction for period t in $T_c(t)$ yields the same hydration degree as reaction for equivalent period t_{eq} in T_r. t_{eq} defined by Eq. (2) is a function of period t, actual temperature $T_c(t)$ and reference temperature T_r.

$$a(t)=\frac{T_{ad}(t)-T_0}{T_{ad}(\infty)-T_0} \tag{1}$$

$$t_{eq}(T_r,t,T_c)=\sum\left(\frac{k_c}{k_r}\right)\Delta t \tag{2}$$

For common chemical reactions, Arrhenius equation in Eq. (3) gives the dependence of the rate constant k on the temperature T and activation energy E (Connors 1990). In Eq. (3), A is a constant independent from temperature, R is the universal gas constant equal to 8.3144 J/(mol • K), and unit of E and T are J/mol and ℃. Hydration of cement is a complicated reaction comprised of reactions of its' compounds. Arrhenius equation is an approximation of dependence of cement hydration reaction on temperature, and activation energy of cement hydration reaction is called "apparent" activation energy E_a, which is affected by fineness of cement compounds, w/c ratio (D'Aloia and Chanvillard 2002, Schindler 2004). According to Jonasson (1994), E_a can be determined by Eq. (4). By substituting Eqs. (3) and (4) into Eq. (2), Eq. (5) is obtained to equivalent age $t_{eq}(T_r,t,T_c)$.

$$k=A\cdot\exp\left(\frac{-E}{R\cdot(273+T)}\right) \tag{3}$$

$$E_a(T)=44066\left(\frac{30}{10+T}\right)^{0.45} \tag{4}$$

$$t_{eq}(T_r,t,T_c)=\sum\exp\left(\frac{1}{R}\left(\frac{E_a(T_r)}{273+T_r}-\frac{E_a(T_c)}{273+T_c}\right)\right)\Delta t \tag{5}$$

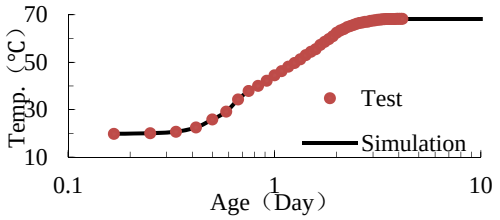

Fig. 3 Simulation and test results of adiabatic temperature of concrete C50

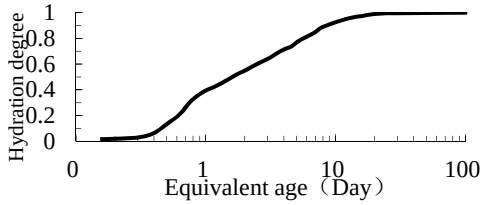

Fig. 4 Equivalent age-hydration degree curve of concrete C50 ($T_r = 20$ ℃)

Based on principles of equivalent age and hydration degree, adiabatic temperature curve of concrete C50 for slab in Fig. 3 is transformed into (EAHDC) in Fig. 4.

In finite element analysis of heat transfer, initial time is t_0 the, and the ith incremental step of duration Δt_i starts at time t_i, and ends at t_{i+1}. Equivalent age $t_{eq}(T_r,t_i,T_c)$ and $t_{eq}(T_r,t_{i+1},T_c)$ corresponding to time t_i, and t_{i+1} can be determined by Eq. (7) and (8) respectively. The hydration degree $a(t_i)$ and $a(t_{i+1})$ can be determined by interpolating EAHDC in Fig. 4 using $t_{eq}(T_r,t_i,T_c)$ and $t_{eq}(T_r,t_{i+1},T_c)$ respectively. The total heat release Q_i from time t_i to t_{i+1} is a function of $a(t_i)$ and $a(t_{i+1})$ defined by Eq. (9), where Q_{sum} is the total heat release of cement in unit volume of concrete. Assume that the variation of temperature in an incremental step is negligible, then the heat release rate dQ_i/dt in the ith incremental step can be determined by Eq. (10).

The cement used has a total heat release of 478.21 kJ/kg, and mix and properties of slab concrete C50 are given in Table 1 and Table 2 respectively. Simulated result of adiabatic test using EAHDC has good agreement with test data as shown in Fig. 3.

Simulation of construction process. The slab, with a volume of 9266 m^3 and 37 oblique layers as shown in Fig. 2, was finished by casting all layers consecutively within 68 hours. The volume of every layer is different from the others as shown in Fig. 5(a), so is the same case with casting time of every layer as shown in Fig. 5(b).

At the time the last layer was finished, the age of the first layer was 68 hours, which means the hydration degree of the first layer was already 97.6% according to EAHDC. Both the differences of age and the differences of hydration degrees among layers reveal that simulation of construction process is necessary. To simulate construction process, the MCIF provided by ABAQUS was applied as following :

(1) 38 analysis steps were created for thermal field analysis. The first 37 were for simulation of construction process. For the first 37 step, the time period of ith step T_{step_i} is the casting time of ith layer as shown in Fig. 5(b).
(2) At the beginning of the first step, layer 2 to 37 were deactivated, only the first layer was activated. At beginning of the second step, layer 2 was activated. Likewise at the beginning of ith step, ith layer was activated.
(3) The 38th analysis step, following the 37th layers, had a time period T_{step_38}, equals to difference between total analysis time and total casting time.

In the simulation of hydration temperature of slab, EAHDC and MCIF are used in combination.

$$t_{eq}(T_r, t_0, T_c) = 0 \tag{6}$$

$$t_{eq}(T_r, t_i, T_c) = \exp\left(\frac{1}{R}\left(\frac{E_a(T_r)}{273+T_r} - \frac{E_a(T_0)}{273+T_0}\right)\right)\Delta t_0 + \cdots + \exp\left(\frac{1}{R}\left(\frac{E_a(T_r)}{273+T_r} - \frac{E_a(T_{i-1})}{273+T_{i-1}}\right)\right)\Delta t_{i-1} \tag{7}$$

$$t_{eq}(T_r, t_{i+1}, T_c) = t_e(T_r, t_{i+1}, T_c) + \exp\left(\frac{1}{R}\left(\frac{E_a(T_r)}{273+T_r} - \frac{E_a(T_i)}{273+T_i}\right)\right)\Delta t_i \tag{8}$$

$$Q_i = Q_{sum}\left(\alpha(t_{i+1}) - \alpha(t_{i+1})\right) \tag{9}$$

$$\frac{dQ_i}{dt} = \frac{Q_{sum}\left(\alpha(t_{i+1}) - \alpha(t_{i+1})\right)}{\Delta t_i} \tag{10}$$

Table 1. Mix and properties of concrete C50 used in slab

compressive strength (MPa)	design slump (mm)	Concrete mix（kg/m^3） water	cement	flashy	ground slag	medium sand	gravel 5-16	gravel 16-31.5	additive
50	180±30	151	240	100	50	780	470	580	3.9

FINITE ELEMENT MODEL (FEM) OF SLAB FOR THERMAL FIELD ANALYSIS

Dimensions of model were shown in Fig. 6. As shown in Fig. 6 and Fig. 7, water proof layer, bed rock and prestressed concrete corridor under slab was included as boundary. Given features of geometry and construction method, half model can be

used. By the same token, quarter model as shown in Fig. 8 can be used for simulation without construction process. The half model and quarter model used the same materiel properties. Based on material used in practice, parameters for thermal analysis of the slab are prescribed in Table 2 (Wang et al. 2010, Zhang et al. 2010), and air temperature during casting is shown in Fig. 9.

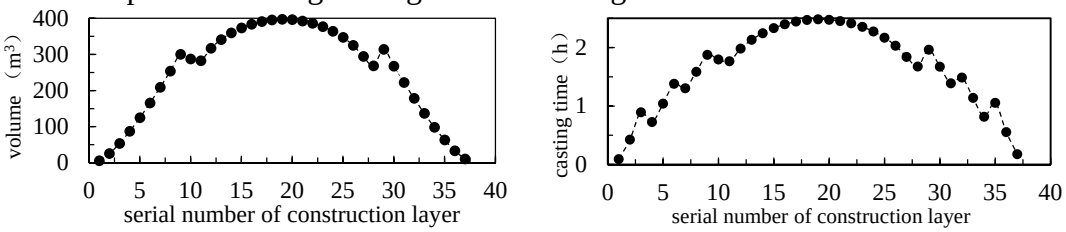

(a) volume of construction layers (b) casting time of construction layers

Fig. 5 Concrete volume and casting time of all construction layers

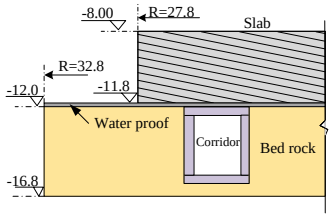

Fig. 6 Diagram of section of slab

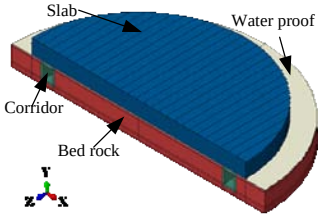

Fig. 7 Half model slab

VALIDATION

Arrangement of gauges and analysis on measured temperature data. Totally 73 temperature gauges are deployed as shown in Fig. 10(a) and (b), and every gauge started measuring as the placement of concrete at its' location. Identifier of every gauge is comprised of a number as horizontal identifier and an alphabet as vertical identifier representing plane location and elevation location respectively in Fig. 10(b). It is worthwhile to notice the gauges were arranged symmetrically about axle of slab. The measured temperature curves of some gauges symmetrical about section 1-1 in Fig. 10 are given in Fig. 11. The fact is apparent in Fig. 11 that curves of every two symmetrical gauges are almost identical, which indicates hydration temperature distributed symmetrical about section 1-1 in the slab.

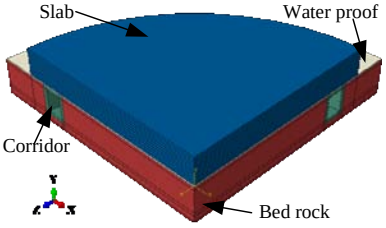

Fig. 8 Quarter model of slab

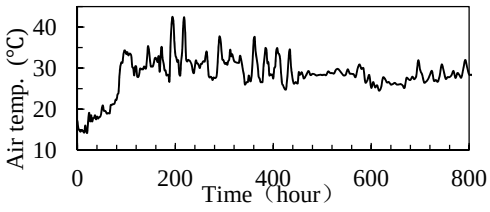

Fig. 9 Measured air temperature during the casting of slab

Validation of EAHDC-MCIF combination method. Concrete casting of the slab initiated at time zero, and temperature of every gauge increased initially as the concrete placement at its' location. For gauges in section 1-1 with vertical identifier A, C and E, the time $T_{initial}$ when temperature increased initially of the measured data and simulated results with/without construction process are given in Fig. 12. When construction process is not simulated, the difference of $T_{initial}$ between simulated

result and measured data of the same point can go up to 51 hours. But when construction process is simulated, the maximum of this difference of $T_{initial}$ is only 3 hours. Fig. 13(a), (b) and (c) are given for comparison of measured and simulated results for points in section 1-1 at elevation A, C and E respectively, and Fig. 14(a) to (f) for for points in section 2-2. Improved accuracy by EAHDC-MCIF combination method is considerable.

Table 2. Properties for thermal analysis of the slab

Material	density (kg/m^3)	conductivity $w/(m \cdot ℃)$	specific heat $J/kg \cdot ℃$	heat exchange coefficient $W/m^2 \cdot ℃$
slab	2400	2.33	900	7.8/3.6/5.4*
water proof	2200	0.15	970	15.0
corridor	2400	2.33	900	15.0
bed rock	3000	2.33	1000	7.8

(*7.8 is for the case when heat exchange between concrete to air directly without insulation effect, 3.6 is for concrete on side surface of slab with insulation of formwork, 5.4 is for concrete on the top surface of slab with insulation of insulating material.)

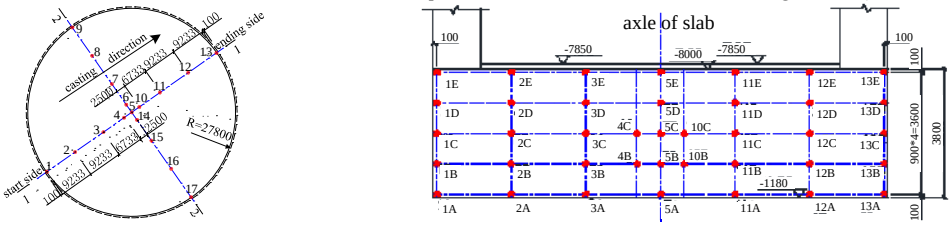

(a) Plan view (b) Elevation view in section 1-1

Fig. 10 Location of gauges inside the slab

(section 2-2 and 1-1 are orthogonal and have identical gauge arrangement, unit: mm)

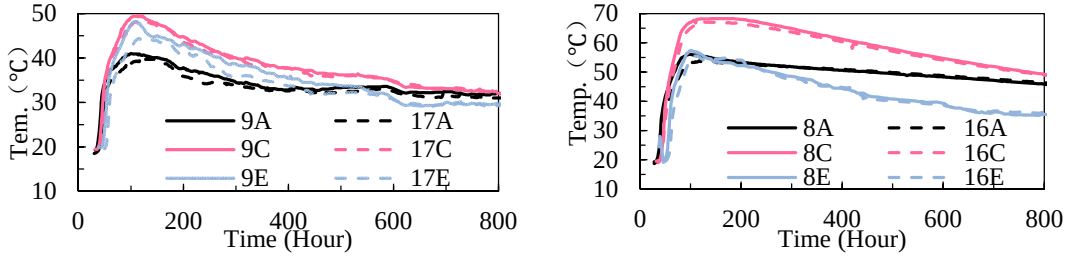

(a) gauges A, C and E on lines 9 and 17 (b) gauges A, C and E on lines 8 and 16

Fig. 11 Measured temperature curves of typical gauges

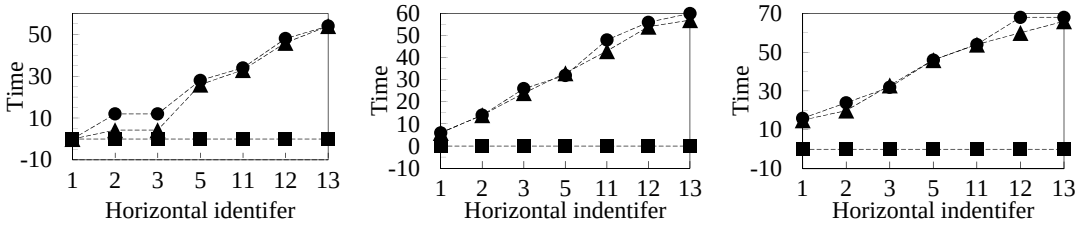

(a) A points (b) C points (c) E points

Fig. 12 Time when temperature increased initially of points in section 1-1

(● measured, ■ and ▲ for simulation with/without construction process respectively)

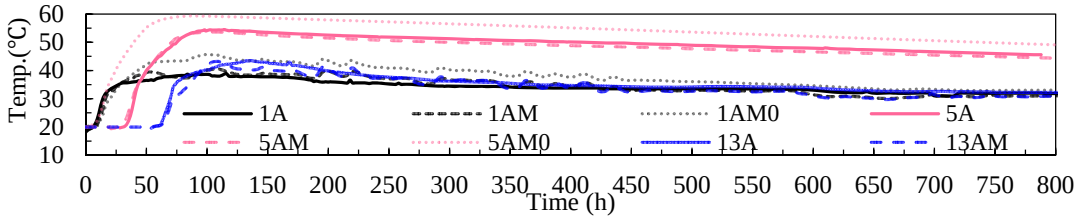

(a) points 1A, 5A and 13A

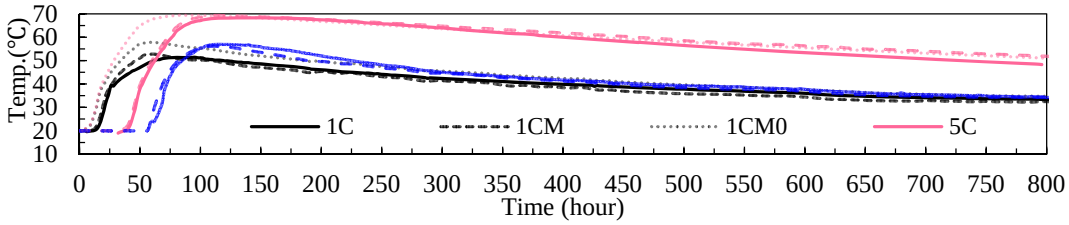

(b) points 1C, 5C and 13C

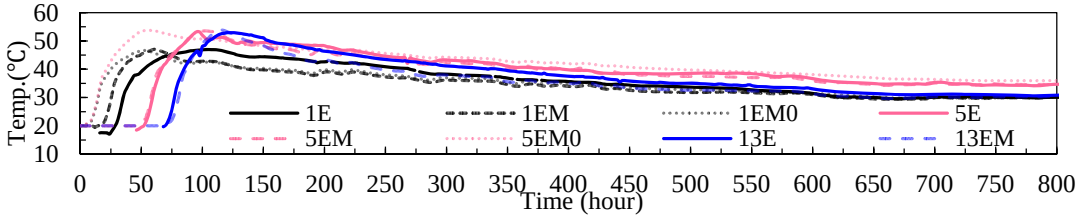

(c) points 1E, 5E and 13E

Fig. 13 Measured and simulated temperture curves of points in section 1-1
(solid lines are measured results, and dash lines taged with M or M0 are simulated results with or without contruction process repectively.)

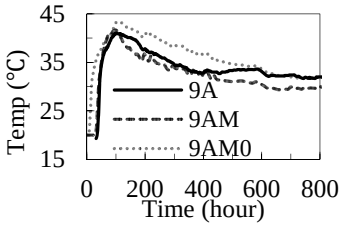

(a) point 9A

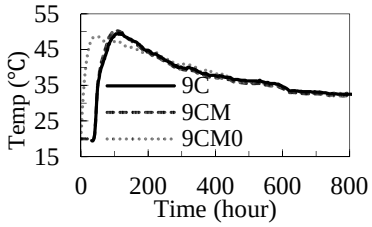

(b) point 9C

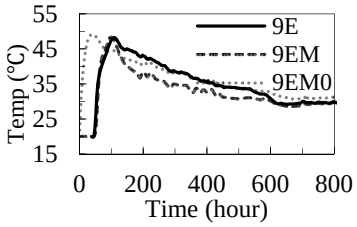

(c) point 9E

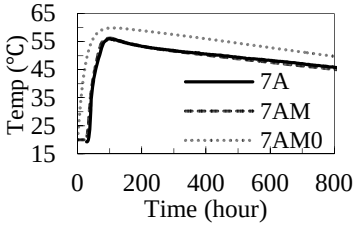

(d) point 7A

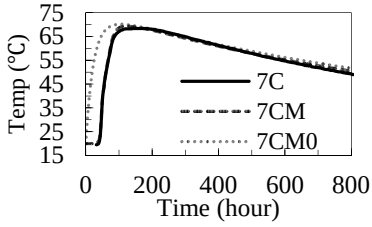

(e) point 7C

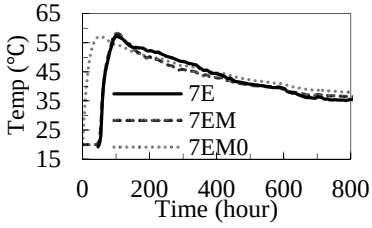

(f) point 7E

Fig. 14 Measured and simulated temperture curves of points in section 2-2
(solid lines are measured results, and dash lines taged with M or M0 are simulated results with or without contruction process repectively.)

CONCLUSION

In simulating hydration temperature field of the slab, following conclusions are drawn: (1) The equivalent age-hydration degree curve (EAHDC) can be used to consider effects of age and temperature on hydration rate of cement. (2) Hydration

temperature field of the slab is symmetrical about section 1-1, and is strongly affected by construction process. (3) With combination of EAHDC and the Model Change Interaction Function(MCIF), the simulated results are quite close to measured data.

ACKNOWLEDGEMENTS

The authors would like to express their gratitude to China State Construction Engineering Corporation (Proj. No. CSCEC2B-2010-K-02). The materials presented are the research findings by the authors only.

REFERENCE

Benboudjema, F. and J. M. Torrenti (2008), "Early-age behaviour of concrete nuclear containments." *Nuclear Eng. and Design*, **238**(10), 2495-2506.

Connors, K. A. (1990). *Chemical kinetics the study of reaction rates in solution*. New York: VCH Publ.

D'Aloia, L. and G. Chanvillard (2002), "Determining the "apparent" activation energy of concrete: Ea—numerical simulations of the heat of hydration of cement." *Cement and Concrete Research*, **32**(8), 1277-1289.

Dimmelmeier, H., J. Eyink and M. A. Movahed (2012), "Computational validation of the EPR™ combustible gas control system." *Nuclear Eng. and Design*, **249**, 118.

Jonasson, J. E., Groth, P., Hedlund, H. (1994), "Modeling of Temperature and Moisture Field in Concrete to Study Early Age Movements as a Basis for Stress Analysis", International Symposium Thermal Cracking in Concrete at Early Ages, *Spon press*. Munchen, Germany

Schindler, A. K. (2004), "Effect of temperature on hydration of cementitious materials." *ACI Mat. J.*, **101**(1), 72-81.

Simulia (2009), Abaqus analysis user's manual, version 6.9, Dassault Systèmes Simulia Corp Providence, RI.

WANG, P., S. FENG and X. LIU (2005), "Research Approaches of Cement Hydration Degree and Their Development." *Journal of Building Materials*, **6**, 1-10.

Wang, Y., X. Zhang, D. Cheng and Z. Zhong (2010), "Thermal stress of mass concrete for foundation of CPR1000 nuclear power plant." *Industrial Construction*, **1**, 11-13.

Weisshäupl, H. (1999), "Severe accident mitigation concept of the EPR." *Nuclear Engineering and Design*, **187**(1), 35-45.

Zhang, Z., X. Li, X. Zhang and D. Cheng (2010), "Finite element analysis and study on curing methods and technical indexes of mass-concrete construction." *Industrial Construction*, **1**, 5-7.

Zhang, Z., H. Song and H. Huang (2003), "New theory on adiabatic temperature rise and heat conduction equation of concrete." *Journal of Hehai University*, **30**(3), 1-6.

Zhu, B. (2003), "A method for computing the adiabatic temperature rise of concrete considering the effect of the temperature of concrete." *Journal of Hydroelectric Engineering*, **2**, 69-73.